Available online at www.sciencedirect.com
ScienceDirect
Nuclear Instruments and Methods in Physics Research A 580 (2007) 282–285
NUCLEAR INSTRUMENTS & METHODS IN PHYSICS RESEARCH Section A
www.elsevier.com/locate/nima

Optimization of filtered neutron beams for the calibration of superheated droplet detectors at the RPI

F. Nascimento[a], A.R. Ramos[b,c,*], A.C. Fernandes[c,d], M. Felizardo[b,c], T. Morlat[c], J.G. Marques[b,c], F. Giuliani[c], T.A. Girard[c], J.A. Paixão[a]

[a]*Fac. Ciencias and Tecnol, Dept. Fis., Univ. Coimbra, 3004-516 Coimbra, Portugal*
[b]*ITN–Instituto Tecnológico e Nuclear, Estrada Nacional 10, 2686-953 Sacavém, Portugal*
[c]*CFN da Universidade de Lisboa, Av. Prof. Gama Pinto 2, 1649-003 Lisboa, Portugal*
[d]*Hospital de Santa Maria, Av. Prof. Egas Moniz, 1649-035 Lisboa, Portugal*

Available online 18 May 2007

Abstract

Superheated droplet detectors (SDDs) have been investigated for applications in neutron dosimetry and spectrometry. Varying the detector temperature, it is possible to change the neutron energy detection threshold of SDDs, thus allowing the use of a single detector to measure neutrons of different energy, without any change of the experimental setup. However, the neutron threshold energy versus temperature curves have to be experimentally determined. The determination of the calibration curves requires the use of monochromatic neutron beams.

The neutron spectrum from a nuclear reactor covers a wide energy range, from meV to several MeV. Beams of quasi-monochromatic neutrons can be generated by filtering neutrons emerging from the core with suitable materials, such as Fe (for 24 keV neutrons) and Si (144 and 54 keV). These materials have windows in their neutron cross-sections, so that neutrons corresponding to these windows are transmitted, whereas neutrons with other energies are attenuated.

We report on the MCNP simulation study of passive monochromators of Si + S and Si + Ti for the production of quasi-monochromatic neutron beams of 54 keV (Si + S) and 144 keV (Si + Ti). The simulations allowed the purity versus intensity of the neutron beams to be optimized, within the geometrical constraints of the beam port.

PACS: 02.70.Lq; 28.20.−v

Keywords: Quasi-monochromatic neutron beams; Superheated droplet detectors

1. Introduction

The neutron spectrum from a nuclear reactor covers a wide energy range, from meV to several MeV. Beams of approximately monoenergetic neutrons can be generated by filtering neutrons emerging from the core of a reactor. Suitable filter materials include iron (24 keV neutrons) and silicon (144 keV and 54 keV neutrons). These materials have "resonance windows" in their cross-sections, so that neutrons with energies corresponding to these windows are transmitted, whilst neutrons with other energies are attenuated. Several references regarding the application of passive monochromators can be found in literature [1,2].

Superheated droplet detectors (SDDs) have been investigated for applications in neutron dosimetry and spectrometry [3]. Varying the detector temperature, it is possible to change the neutron energy detection threshold of SDDs, thus allowing the use of a single detector to measure neutrons of different energy, without any change of the experimental set up. However, the neutron threshold energy versus temperature curves have to be experimentally determined. The determination of the calibration curves requires the use of monochromatic neutron beams.

This work describes the Monte Carlo simulation of passive monochromators to be installed in the fast beam

*Corresponding author. Tel.: +351 21 994 6126; fax: +351 21 994 1039.
E-mail address: ariel@itn.pt (A.R. Ramos).

0168-9002/$ - see front matter
doi:10.1016/j.nima.2007.05.156

tube facility of the Portuguese Research Reactor (RPI), for use in SDD calibration.

2. Facility description

RPI is a swimming pool type reactor with a maximum power of 1 MW and a maximum thermal neutron flux at the core of about 2×10^{13} n/cm^2/s. The fast beam facility (Fig. 1) is a dedicated dry irradiation facility built around one of the beam tubes, with an irradiation chamber with 100 cm × 60 cm × 60 cm ($l \times w \times h$) at the end of the tube, as well as a prolongation inside the beam tube, made through the introduction of a 100 cm long cylinder with 150 mm inner diameter, attached to the face of the beam tube housing. The neutron beam size is 150 mm, as defined by the diameter of the beam tube close to the core. Shielding of the facility is done by a combination of polyethylene lined with Cd and high-density concrete. A Pb filter and a Boral filter were placed inside the irradiation tube to reduce the gamma field and the thermal neutron component, respectively. Further details can be found in Refs. [4,5].

To minimize changes to the existing facility and maintain its versatility, the passive monochromators will be installed in the 100 cm long cylinder attached to the face of the beam tube housing, as indicated in Fig. 1. This is the origin of the major geometric constraint of the design: the maximum monochromator length should not exceed 100 cm.

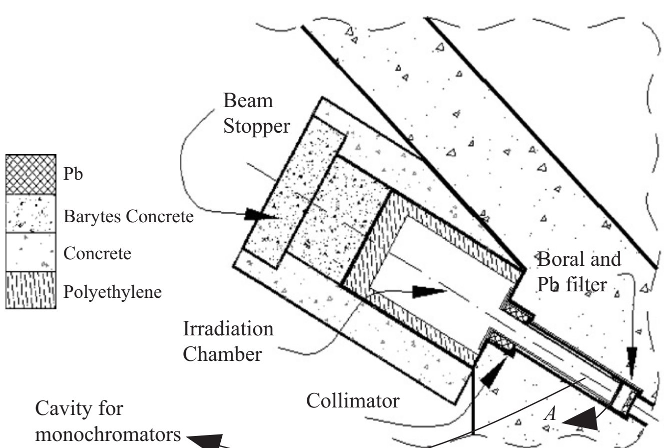

Fig. 1. Horizontal cut of the fast neutron facility. For simplification the outer radiation shielding is not shown complete.

3. Monte Carlo simulation

3.1. The source term

The radiation field in the beam port was calculated with the Monte Carlo Code MCNP—4C and adjusted to measurements performed with various activation foils Ref. [6]. The radiation field determined in Ref. [6] for position A in Fig. 1 was used as the source term in the present work. The source was taken as a circular disk positioned in A, emitting perpendicular to its surface.

3.2. The passive monochromators

We simulated different monochromator geometries, in order to maximize intensity and purity of the filtered beams. The filter and beam port geometry were simulated without approximations using the Monte Carlo code MCNP—4C. The number of histories was chosen in order to obtain an error lower than 10%. All of the statistics checks of MCNP were passed successfully. Fig. 2 shows a typical monochromator arrangement. The arrangement is composed of a primary filter, Si, with windows in its cross-section at 144 and 54 keV. The secondary filter is either S, to close the cross-section window at 144 keV and allow the transmission of 54 keV neutrons, or Ti, to close the cross-section window at 54 keV and allow the transmission of 144 keV neutrons. In Fig. 2, the first two Si cylinders have 2.5 cm diameter. The last Si and the Ti cylinders have 2 cm diameter. The final Pb cylinder has a 2 cm hole. Simulation data shown in this work correspond to a MCNP tally in a cylindrical cell 2 cm in diameter, placed at the exit of the monochromator.

4. Results

Given the beam port physical restrictions, two different types of filter geometries were considered. In the first case, the primary filter (Si) length remained constant, and the secondary filter length (Ti or S) varied. In the second case, the total filter length was kept constant and the length of both primary and secondary filter varied. For the case of

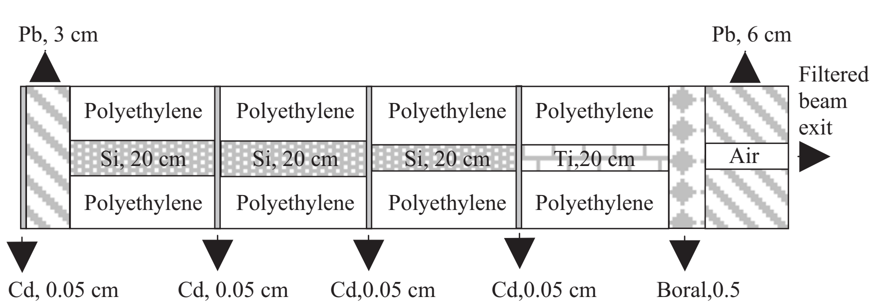

Fig. 2. Typical arrangement for a monochromator. The example shown is for a Si + Ti filter for 144 keV neutron transmission.

Table 1
Summary of the different filter configurations studied

Filter configuration	Peak (keV)	Purity (%)	Energy spread (keV)	Peak flux (n/MeV)
Constant Ti (Si + Ti)				
60 cm Si + 19.2 cm Ti	144	72	22	1.14×10^{-3}
65 cm Si + 19.2 cm Ti	144	76	20	1.08×10^{-3}
69.5 cm Si + 19.2 cm Ti	144	76	20	1.03×10^{-3}
Constant Si (Si + Ti)				
65 cm Si + 5 cm Ti	144	61	25	2.91×10^{-3}
65 cm Si + 10 cm Ti	144	68	23	2.04×10^{-3}
65 cm Si + 19.2 cm Ti	144	76	20	1.08×10^{-3}
Constant total length (Si + Ti)				
65 cm Si + 19.2 cm Ti	144	76	20	1.08×10^{-3}
55 cm Si + 29.2 cm Ti	144	76	23	5.63×10^{-4}
45 cm Si + 39.2 cm Ti	144	76	23	3.38×10^{-4}
Constant Si (Si + S)				
65 cm Si + 5 cm S	54	26	2	1.84×10^{-2}
65 cm Si + 10 cm S	54	35	2	1.72×10^{-2}
65 cm Si + 19.2 cm S	54	47	2	1.53×10^{-2}
Constant total length (Si + S)				
65 cm Si + 19.2 cm S	54	47	2	1.53×10^{-2}
55 cm Si + 29.2 cm S	54	42	2	1.44×10^{-2}
45 cm Si + 39.2 cm S	54	31	2	1.45×10^{-2}

Purity is the ratio of neutrons present in the energy region of the FWHM of the peak to all neutrons. Energy spread is the FWHM.

the Si + Ti filter, a third geometry was analyzed, in which the secondary filter length was kept constant and the primary filter length varied. Table 1 summarizes the main results obtained.

4.1. *Si + Ti (144 keV)*

As seen in Table 1, for a fixed Ti length, increasing the Si increases beam purity up to a Si length of 65 cm. Increasing the Si further does not result in increased purity or smaller beam energy spread. The fast ($E > 1$ MeV) neutron component of the filtered spectrum (not shown in Table 1) decreases with increasing Si length. The thermal ($E < 1$ eV) neutron component (not shown) is low, corresponding in all cases to less than 2% of the total filtered spectrum.

For a fixed Si length, increasing the Ti results in increased beam purity and decreased beam energy spread. The fast neutron component of the beam also decreases with increasing Ti. The beam intensity also decreases.

For a fixed total filter length (~84 cm), decreasing the Si length while increasing the Ti does not affect beam purity, but the energy spread of the beam increases with decreasing Si. Also, the peak intensity decreases with decreasing Si length.

4.2. *Si + S (54 keV)*

For a fixed Si length, increasing the S does not affect the beam energy spread, but increases purity and decreases the fast neutron component of the beam. The beam intensity also decreases slightly.

For a fixed total filter length (~84 cm), decreasing the Si length and increasing the S decreases beam purity, only slightly decreasing the intensity.

5. Discussion

Given the results presented above, the best geometry studied is, for the Si + Ti filter, 65 cm Si + 19.2 cm Ti. In this case, the simulations indicate a beam purity of 76%, with a thermal neutron component of 1% and a fast neutron component of 3%.

For the Si + S filter, the best geometry is 65 cm Si + 19.2 cm S. In this case, the simulations indicate a beam purity of 47%, with a thermal neutron component of less than 2% and a fast neutron component of 7%. Note that, as it is defined in Table 1, beam purity is related to the number of neutrons with energies in the interval [E-FWHM/2; E + FWHM/2]. As the Si + S filter has a very small beam energy spread (2 keV), the purity value is low. Considering a 15 keV energy range around the 54 keV peak, the purity value for the chosen Si + S geometry is 63%. This is still a low value, indicating that the Si + S filter performance, as regards purity, is inferior to the Si + Ti filter. The intensity of the Si + S 54 keV peak will, however, be much higher than the Si + Ti 144 keV peak.

Fig. 3 shows the neutron spectra per lethargy unit of the best Si + Ti and Si + S geometries. For comparison, the

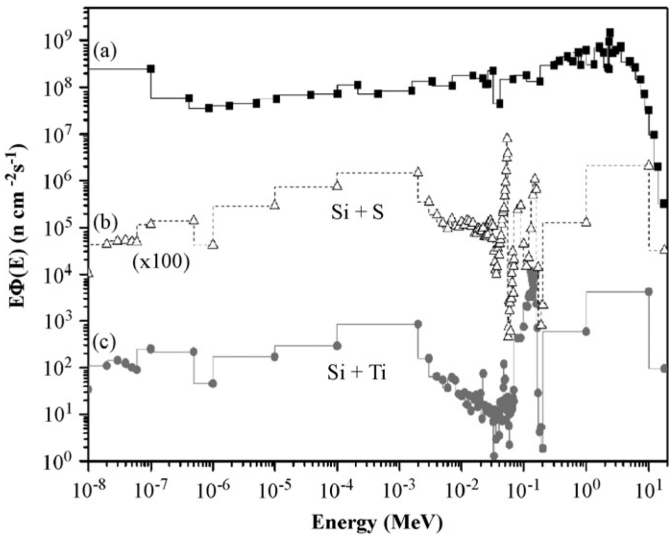

Fig. 3. Neutron spectra per lethargy unit: (a) before the filter, inside the cylindrical cavity, at the point closest to the core (point *A* in Fig. 1); (b) at the exit of the Si + S filter (65 cm Si + 19.2 cm S); (c) at the exit of the Si + Ti filter (65 cm Si + 19.2 cm S).

neutron spectrum in the filter cavity, before the filter material, is also included.

For application in SDD calibration, an important feature of the filtered neutron beams is the fast neutron component. The simulations indicate that both chosen filter geometries have reduced fast neutron components, thus making them appropriate for the envisaged application. Another important feature is the gamma component of the beam. Simulation work related to the analysis of the gamma component will be the object of a separate publication.

6. Conclusions

We reported the MCNP optimization study of Si + S and Si + Ti neutron filters for the production of quasi-monochromatic neutron beams of 54 keV (Si + S) and 144 keV (Si + Ti). The simulations allowed the purity versus intensity of the neutron beams to be optimized, within the geometrical constraints of the beam port.

Acknowledgments

This work was partly supported by grant POCTI/FIS/55930/2004 of the Foundation for Science and Technology of Portugal, co-financed by FEDER.

References

[1] C.A. Perks, K.G. Harrison, R. Birch, H.J. Delafield, Radiat. Prot. Dosim. 15 (1986) 31.
[2] A. Michandon, S. Cierjacks, R.E. Chrien (Eds.), Neutron Sources for Basic Physics and Applications, Pergamon Press, New York, 1983 (Chapter 8).
[3] R.E. Apfel, S.C. Roy, Nucl. Instr. and Meth. in Phys. Res. 219 (1984) 582.
[4] F.J. Franco, Y. Zong, J.A. De Agapito, J.G. Marques, A.C. Fernandes, J. Casas-Cubillos, M.A. Rodriguez-Ruiz, Nucl. Instr. and Meth. A 553 (2005) 604.
[5] A. Vieira, A. Ramalho, I.C. Gonçalves, A. Fernandes, N. Barradas, J.G. Marques, J. Prata, Ch. Chaussy, in: A. Kling, et al. (Eds.), Proceedings of MC 2000 Conference on Advanced Monte Carlo for Radiation Physics, Particle Transport Simulation and Applications, Springer, Heidelberg, 2000, p. 943.
[6] A.C. Fernandes, I.C. Gonçalves, J.G. Marques, J. Santos, A.J.G. Ramalho, M. Osvay, in: J. Wagemans, H. Aït Abderrahim, P. D'hondt, C. De Raedt (Eds.), Proceedings of the 11th Conference on Reactor Dosimetry, World Scientific, Brussels, 2003, p. 143.